

α -cluster structure of the yrast bands of ^{44}Ti

J. Zhang,* W. D. M. Rae, and A. C. Merchant

Department of Physics, University of Oxford, Nuclear Physics Laboratory, Keble Road, Oxford OX1 3RH, United Kingdom

(Received 27 April 1995)

The Bloch-Brink microscopic α -cluster model is used to investigate the structure of the positive and negative parity yrast bands of ^{44}Ti . Unlike the resonating group method or the local potential model, we approximate the wave function of ^{44}Ti by an intrinsic configuration which is obtained from a variational principle. States with good angular momenta are constructed using angular momentum projection techniques. The wave function is completely antisymmetrized and the center of mass motion is treated properly. The calculated $E2$ transition strengths reproduce experiment very well, but the energy spectra are in a poor agreement with the data.

PACS number(s): 21.60.Gx, 23.20.Js, 23.20.Lv, 27.40.+z

I. INTRODUCTION

It has been well established that the positive and negative parity yrast bands in ^{44}Ti can be described using α - ^{40}Ca cluster models. Numerous calculations [1–7] reproduce the experimentally observed positive parity band terminated by a $J^\pi=12^+$ level at 8.04 MeV. All the models predict a negative parity band, often termed an *inversion doublet*. Indeed, the first few states of a negative parity yrast band have been found recently [8,9] and fit nicely into the theories.

The peculiar and intriguing feature of the yrast bands of ^{44}Ti is that the energy spectra, and the intraband $E2$ transition strengths in the positive parity band, deviate substantially from the prediction of an axial rigid rotor model. This nucleus appears to be a rotor with a changing moment of inertia but the puzzle is that the decreasing energy gap as a function of angular momentum indicates a stretching rotor while the diminishing $B(E2)$ values would imply a shrinking rotor. This abnormality, very similar to what is observed in ^{20}Ne [10], is not yet fully understood.

Calculations concerning the α -cluster structure of ^{44}Ti can all be classified into two groups: microscopic models and phenomenological local-potential models. In a microscopic calculation one usually uses either the shell model or the resonating group method (RGM). The shell model assumes that four nucleons occupy the $f_{7/2}$ subshell. This is basically a truncated configuration-interaction calculation and it has been shown to give correct $B(E2)$ values only when large effective charges ($\delta e = 0.5e$) are used [2]. The RGM [1,3] is more flexible in that the wave functions for the constituent clusters are specified microscopically and the relative motion can in principle be solved variationally. To simplify the calculation, one usually takes the wave functions for α and ^{40}Ca to be, respectively, the configurations $(0)^4$ and $(0)^4(1)^{12}(2)^{24}$ where the numbers in parentheses are the total quanta of a single particle harmonic oscillator wave function. A numerically less difficult yet physically more intuitive approach is the binary local potential model (LPM) which, as

initially proposed by Buck *et al.* [11], assumes that the interaction between two clusters is described by a local potential and the clusters retain their free space properties.

In the calculations presented here the wave function of ^{44}Ti is specified microscopically using the Bloch-Brink α -cluster model [12]. No intercluster potential is introduced but rather an effective two-body nucleon-nucleon interaction, the Brink-Boeker $B1$ force [13], is used throughout the calculation. The Coulomb force is also included. We compare our results with those of Friedrich and Langanke [1].

II. α -CLUSTER WAVE FUNCTIONS FOR ^{44}Ti

The Bloch-Brink (BB) α -cluster model is well documented; we refer the interested reader to the original paper by Brink [12].

The cluster geometry of ^{40}Ca has been recently computed [1,14] and it can be accurately represented by a regular tetrahedron with three α -clusters on each edge. Minimization of the total binding energy of ^{40}Ca yields a distance between two adjacent clusters of 1.25 fm and the oscillator frequency common to all α clusters in the configuration is such that $\hbar\omega_0 = 11.2$ MeV.

A recent completely unconstrained variational calculation [15] shows that the intrinsic configuration of the ground state of ^{44}Ti is reminiscent of an α - ^{40}Ca structure. In the same paper the energy spectrum of the positive parity band has been also computed using the cranking approximation [16,17] and familiar results such as centrifugal antistretching effects on the cluster geometry and deviation of the energy spectrum from that of a rigid rotor model are obtained. Ideally, the model should be subject to more stringent tests, for example, by comparing theoretical intraband $B(E2)$ values with the experimental results, but the cranking approximation on its own does not allow such calculations. To calculate $B(E2)$'s one has no choice but to perform angular momentum projection. In the context of angular momentum projection variation after projection is always preferable. Unfortunately, such a calculation for a nucleus as heavy as ^{44}Ti is too time consuming; the reason is that there are in this case

*Permanent address: Shanghai Institute of Nuclear Research, P.O. Box 800-204, Shanghai, China.

28 coordinate parameters to vary, far too many even for a modern workstation.

To make the problem tractable we approximate the cluster geometry by an α plus ^{40}Ca structure. We shall as usual impose the condition that each α cluster has the same ω_0 so that spurious center of mass motion is not a problem. We construct the wave function of ^{44}Ti by putting an extra α cluster on a continuation of one of the lines joining an apex to the center of the opposite face of the ^{40}Ca tetrahedron. The reason that we choose this arrangement is because of all possible orientations of the tetrahedron at a certain α - ^{40}Ca distance, which we call D , the above-mentioned geometry is found invariably to give the maximum binding energy. We do not constrain the tetrahedron size or ω_0 to have the same values as in the ^{40}Ca case; instead, we calculate the binding energy of the intrinsic configuration as specified above for various D 's, ω_0 's, and the sizes of the tetrahedron. It is found that for a given D there are certain values of ω_0 and the tetrahedron size that maximize the binding energy. For all values of D the optimized tetrahedron size is very close to that of ^{40}Ca and the optimized ω_0 corresponds to $\hbar\omega_0=11.6$ MeV, exactly in agreement with the well-known formula [18]

$$\hbar\omega_0(A) = \frac{41}{A^{1/3}} \text{ (MeV)}. \quad (1)$$

For this reason, and also to further facilitate our calculation, we therefore fix the ω_0 and the tetrahedron size to the above values, leaving D the only variational parameter.

III. VARIATION AFTER PROJECTION

We then perform exact angular momentum projection [19] along with parity projection at various values of D . Because the assumed intrinsic configuration possesses a threefold symmetry (C_3), the allowed K^π values satisfy [10]

$$K^\pi = 0^\pm, 3^\pm, 6^\pm, \dots \quad (2)$$

We check the K -mixing matrix elements at all D 's. They are found to be negligibly small so that we may ignore K mixing.

Figure 1 shows the projected binding energies vs D for

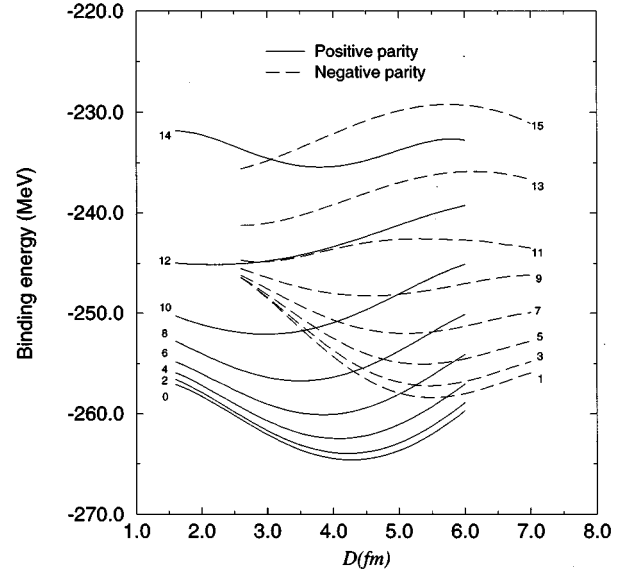


FIG. 1. The binding energies of projected states with good angular momenta; see text for details.

different J^π . In the positive parity case all levels up to $J^\pi=14^+$ have minima at some D 's. The calculated minimum for $J^\pi=14^+$ becomes very tenuous and this is not inconsistent with the fact that the observed positive parity band terminates at $J^\pi=12^+$. In the negative parity case there are minima for levels up to $J^\pi=11^-$. Higher levels do not have a minimum at all. It is seen that the values of D at the minima monotonically decrease with angular momentum for both parities. It is also obvious that the negative parity band has a much larger intercluster separation, especially for the lower angular momentum members. The optimized D for both 1^- and 3^- is 5.5 fm while the sum of the experimentally determined radii of α and ^{40}Ca is 5.16 fm [20]. This probably means that an α - ^{40}Ca cluster model is more appropriate for the negative parity band.

We associate each J^π with a value of D that maximizes the binding energy of that J^π value and then compute intraband $B(E2)$'s using the angular-momentum-projected wave functions. In Table I we have listed the calculated $B(E2)$ values and the optimized α - ^{40}Ca distances. We also make a

TABLE I. Calculated intraband $B(E2;J+2 \rightarrow J)$ values and optimized α - ^{40}Ca distances. BE=binding energy, RM=rotor model.

$K^\pi=0^+$ band						$K^\pi=0^-$ band					
J	$D(J)$ fm	BE MeV	$B(E2;J+2 \rightarrow J)$ ($e^2\text{fm}^4$)			J	$D(J)$ fm	BE MeV	$B(E2;J+2 \rightarrow J)$ ($e^2\text{fm}^4$)		
			Expt.	Theor.	RM ^a				Calc. ^b	Theor.	RM ^a
0	4.3	264.76	120 ± 37	145.5	120.0	1	5.5	258.41	264.7	376.6	376.6
2	4.2	264.11	277 ± 55	190.9	171.4	3	5.5	257.22	279.1	442.3	443.7
4	4.0	262.58	157 ± 28	185.6	188.8	5	5.3	255.08	243.6	365.2	473.1
6	3.8	260.17	>14	164.2	197.7	7	5.1	252.03	184.5	277.1	489.7
8	3.5	256.73	138 ± 28	127.4	203.0	9	4.5	248.26	118.1	116.4	500.3
10	3.0	252.05	<60	63.5	206.6	11	2.9	244.88	54.9		507.7
12	1.8	245.16			209.2						

^aPrediction of a rotor model for $B(E2;J+2 \rightarrow J)$; see text for details.

^bTaken from the calculation of Michel *et al.* [4].

comparison for $B(E2)$ values with the calculation of Michel *et al.* [4] and with experimental data in the case of the positive parity band. The normal free space charges are used in our calculation; no renormalization is required. The calculated $E2$ transitions reproduce the experimental result very well in the positive parity case. We also have calculated intraband $B(E2)$ values for the negative parity band but so far there is no experimental data to compare with. In passing we note that the BB model predicts identically vanishing $E1$ transition strengths which would otherwise link the positive and negative parity yrast levels. Experimentally, no such transitions are observed. The reason why $E1$ is always zero is that the $E1$ transition matrix element is actually the expectation value of the center of charge which is identical to the center of mass in the BB α -cluster model as applied to $A=4N$ self-conjugate nuclei.

Assuming pure $K^\pi=0^\pm$ bands, we also calculate rotor model prediction for $B(E2)$'s (see Table I) of both parity bands according to [21]

$$B(E2; I+2 \rightarrow I) = \frac{5}{16\pi} Q_0^2 \langle 20IK | I+2K \rangle^2. \quad (3)$$

The intrinsic quadrupole moment Q_0 is chosen to give the correct value for the observed $B(E2; 2_1^+ \rightarrow 0_1^+)$ in the positive band case or the calculated $B(E2; 3_1^- \rightarrow 1_1^-)$ in the negative band case.

IV. SUMMARY

Using the BB model we have calculated properties of the lowest positive and negative parity bands in ^{44}Ti . Our calculated intraband $B(E2)$ values for the positive parity band are in good agreement with the observed results, but the calculated energy levels, although deviating from a rigid rotor in a direction required by the data, still exhibit a large discrepancy with experiment. As a matter of fact, all but one calculation from those that have been done to date predict much too large energy gaps for the higher J^π levels. The recent calculation by Buck *et al.* [7] improves somewhat on this

situation by introducing a novel parametrization of the local potential consisting of a linear combination of Woods-Saxon and cubed Woods-Saxon terms. The microscopic reason why such a potential reproduces the data has yet to be investigated.

Our calculations are similar to those of Friedrich and Langanke [1]. The main difference is that in Ref. [1] they essentially used an exactly spherical ^{40}Ca by taking a very small intercluster spacing for the ^{40}Ca tetrahedron. We have taken a different approach and fixed the tetrahedron size by minimizing the total energy before projection. Our calculation reproduces the parity splitting and the $B(E2)$ values quite well at the expense of the energy spectrum which is reproduced better by the calculations of Friedrich and Langanke [1]. We attempted to take the same shell model limit as Ref. [1], but since we include the Coulomb force exactly, our calculation becomes numerically unstable. For this reason we switched off the Coulomb interaction and repeated our calculations using the same ^{40}Ca tetrahedral arrangement of Ref. [1]. The result obtained was very similar to that in Ref. [1], and we found a strongly reduced parity splitting of typically less than 0.5 MeV. To understand the origin of the parity splitting, the calculation was repeated using our previous finite ^{40}Ca tetrahedral dimension, but without the Coulomb interaction. The parity splitting then shows up strongly once more (typically 5–6 MeV). It appears that the finite size of the ^{40}Ca tetrahedron has played a significant role. We emphasize that this is the chief difference between the present calculation and that in Refs. [1,5]. As already noticed [1,5], the calculated 0^+ energy using the Brink-Boeker ($B1$) force is above the $\alpha + ^{40}\text{Ca}$ threshold by some 7 MeV. The calculations [5] using the Hasegawa-Nagata-Yamamoto force and the Volkov $V1$ force gave energies in much better agreement with experiment. This defect of the $B1$ force does not affect the conclusion of the present study. We conclude that to obtain all the features of the data it may be necessary to vary all parameters after angular momentum projection. However, it will immediately become a far more complicated calculation than the one presented here and it will still be difficult to include the Coulomb interaction exactly.

-
- [1] H. Friedrich and K. Langanke, Nucl. Phys. **A252**, 47 (1975).
 [2] K. Itonaga, Prog. Theor. Phys. **66**, 2103 (1981).
 [3] H. Horiuchi, Prog. Theor. Phys. **73**, 1172 (1985).
 [4] F. Michel, G. Reidemeister, and S. Ohkubo, Phys. Rev. Lett. **57**, 1215 (1986); Phys. Rev. C **37**, 292 (1988).
 [5] T. Wada and H. Horiuchi, Phys. Rev. C **38**, 2063 (1988).
 [6] A.C. Merchant, K.F. Pal, and P.E. Hodgson, J. Phys. G **15**, 601 (1989).
 [7] B. Buck, A.C. Merchant, and S.M. Perez, Phys. Rev. C **51**, 559 (1995).
 [8] T. Yamaya, S. Oh-Ami, M. Fujiwara, T. Itahashi, K. Katori, M. Tosaki, S. Kato, S. Hatori, and S. Ohkubo, Phys. Rev. C **42**, 1935 (1990).
 [9] P. Guazzoni, M. Jaskola, L. Zetta, C.-Y. Kim, T. Udagawa, and G. Bohlen, Nucl. Phys. **A564**, 425 (1993).
 [10] A. Arima, H. Horiuchi, K. Kubodera, and N. Takigawa, Adv. Nucl. Phys. **5**, 345 (1972).
 [11] B. Buck, C.B. Dover, and J.P. Vary, Phys. Rev. C **11**, 1803 (1975).
 [12] D.M. Brink, in *The Alpha-Particle Model of Light Nuclei*, Proceedings of the International School of Physics "Enrico Fermi," Course XXXVI, Varenna, 1966, edited by C. Bloch (Academic Press, New York, 1966), p. 247.
 [13] D.M. Brink and E. Boeker, Nucl. Phys. **A91**, 1 (1967).
 [14] W.D.M. Rae and J. Zhang, Mod. Phys. Lett. A **9**, 599 (1994).
 [15] J. Zhang, W.D.M. Rae, and A.C. Merchant, Nucl. Phys. **A575**, 61 (1994).
 [16] E. Caurier and B. Grammaticos, J. Phys. G **9**, L125 (1983).
 [17] W.D.M. Rae and S. Marsh, Phys. Lett. **161B**, 251 (1985).
 [18] S.A. Moszkowski, Handb. Phys. **39**, 411 (1957).
 [19] R.E. Peierls and J. Yoccoz, Proc. Phys. Soc. London A **70**, 381 (1957).
 [20] R.C. Barrett and D.F. Jackson, *Nuclear Size and Structure* (Clarendon, Oxford, 1977), p. 146.
 [21] P. Ring and P. Schuck, *The Nuclear Many-Body Problem* (Springer-Verlag, New York, 1980), p. 25.